

Enhancement of Magneto-Optic Effects via Large Atomic Coherence

V. A. Sautenkov^{1,5}, M. D. Lukin², C. J. Bednar^{1,3}, G. R. Welch¹, M. Fleischhauer^{1,4},
V. L. Velichansky^{1,5}, and M. O. Scully^{1,3}

¹*Department of Physics, Texas A&M University, College Station, Texas 77843-4242,*

²*ITAMP, Harvard-Smithsonian Center for Astrophysics, Cambridge, MA 02138,*

³*Max-Planck-Institut für Quantenoptik, Garching, D-85748, Germany,*

⁴*Sektion Physik, Universität München, D-80333 München, Germany*

⁵*Lebedev Institute of Physics, Moscow, Russia*

(May 8, 2001)

Abstract

We utilize the generation of large atomic coherence to enhance the resonant nonlinear magneto-optic effect by several orders of magnitude, thereby eliminating power broadening and improving the fundamental signal-to-noise ratio. A proof-of-principle experiment is carried out in a dense vapor of Rb atoms. Detailed numerical calculations are in good agreement with the experimental results. Applications such as optical magnetometry or the search for violations of parity and time reversal symmetry are feasible.

PACS numbers 42.50.-p, 42.50.Gy, 07.55.Ge

Resonant magneto-optic effects such as the nonlinear Faraday and Voigt effects [1,2] are important tools in high-precision laser spectroscopy. Applications to both fundamental and applied physics include the search for parity violations [3,4] and optical magnetometry. In this Letter, we demonstrate that the large atomic coherence associated with Electromagnetically Induced Transparency (EIT) [5,6] in optically thick samples can be used to enhance nonlinear-Faraday signals by several orders of magnitude while improving the fundamental signal-to-noise ratio.

There exists a substantial body of work on nonlinear magneto-optical techniques [1,2,4,7–11], which have been studied both in their own right and for applications. Such techniques can achieve high sensitivity in systems with ground-state Zeeman sublevels due to the narrow spectroscopic features associated with coherent population trapping [12]. The ultimate width of these resonances is determined by the lifetime of ground-state Zeeman coherences, which can be made very long by a number of methods (buffer gases and/or wall coating [4,11,13] in vapor cells, or atomic cooling or trapping techniques). These resonances are easily saturated, however, and power broadening deteriorates the resolution even for very low light intensities. For this reason, earlier observations of nonlinear magneto-optic features used small light intensities and optically thin samples, which corresponds to a weak excitation of Zeeman coherences. Recently, remarkable experiments of Budker and co-workers demonstrated an excellent performance of the magneto-optic techniques in this regime: very narrow magnetic resonances were observed in a cell with a special paraffin coating [4] (effective Zeeman relaxation rate $\gamma_0 \sim 2\pi \cdot 1\text{Hz}$).

This Letter shows that by increasing atomic density and light power simultaneously the magneto-optic signal can be enhanced substantially and the fundamental noise (shot noise) can be greatly reduced. A nearly maximal Zeeman coherence generated under these conditions preserves the transparency of the medium despite the fact that the system operates with a density-length product that is many times greater than that appropriate for $1/e$ absorption of a weak field. At the same time this medium is extraordinarily dispersive [14,15], such that even very weak magnetic fields lead to a large magneto-optic rotation. This effect

is of the same nature as those resulting in ultra-low group velocities [16]. Our experimental results show a potential for several orders of magnitude improvement over the conventional thin-medium–low-intensity approach.

Typical measurements of the nonlinear Faraday effect involve an ensemble of atoms with ground-state Zeeman sublevels interacting with a linearly polarized laser beam. In the absence of a magnetic field, the two circularly-polarized components generate a coherent superposition of the ground-state Zeeman sublevels corresponding to a dark state. A weak magnetic field B applied to such an atomic ensemble causes a splitting of the sublevels and induces phase shifts ϕ_{\pm} which are different for right (RCP) and left (LCP) circularly polarized light. Hence, as linearly polarized light passes through the medium, the direction of polarization changes by an angle ϕ due to the differing changes in the phase of the two circular components.

In our experiment, shown schematically in Fig. 1, an external cavity diode laser (ECDL) was tuned to the 795 nm $F = 2 \rightarrow F' = 1$ transition of the ^{87}Rb D₁ absorption line. The laser beam was collimated with a diameter of 2 mm and propagated through a 3 cm long magnetically shielded vapor cell placed between two crossed polarizers. The cell was filled with natural Rb and a Ne buffer gas at a pressure of 3 Torr. The laser power was 3 mW at the cell entrance. The cell was heated to produce atomic densities of ^{87}Rb near 10^{12} cm^{-3} . A longitudinal magnetic field was created by a solenoid placed inside the magnetic shields and was modulated at a rate of about 10 Hz. The ground state relaxation rate was measured by decreasing sufficiently the laser power, decreasing the density until the absorption was low, and using RF-optical double resonance techniques. The measured value of $\gamma_0 \approx 2\pi \cdot 5 \text{ kHz}$ (FWHM) is attributed to time-of-flight broadening as well as to a residual inhomogeneous magnetic field. The frequency scale of the magnetic resonance was also determined by using an RF-optical double resonance method.

Figure 2 shows the result of direct measurement of the laser intensity at the photo-detector after transmission through the system of two crossed polarizers ($\theta = 45$ degrees) and a vapor cell. We emphasize that no lock-in detection has been used for the data shown in

Fig. 2 whereas in typical nonlinear Faraday measurements sophisticated detection techniques are usually required to obtain a reasonable signal-to-noise ratio. We note that magneto-optical rotation angles increase with optical density as does the slope $\partial\phi/\partial B$ (curves a and b in Fig. 2). The latter increase is the essence of the method being described. Under the present conditions, rotation angles up to 0.7 radians have been observed (curve b) with a good signal-to-noise ratio. For very high densities the absorption becomes large and the amplitude of the magneto-optic signal does not grow with density any further (curve c).

From our measurements of the rotation angles we obtain, for the conditions outlined above:

$$\partial\phi/\partial B = 1.8 \times 10^2 \text{rad/G} . \quad (1)$$

To put this result in perspective, we can estimate the shot-noise limited sensitivity of this medium. The fundamental photon-counting error accumulated over a measurement time t_m scales inversely with the output intensity. That is, for a laser frequency ν [4]

$$\Delta\phi_{err} \sim \sqrt{\hbar\nu/[P(L)t_m]} \quad (2)$$

where $P(L)$ is the power transmitted through the cell. Combining this with our measured rotation angles implies a shot-noise limited sensitivity $B_{min} = \Delta\phi_{err}/(\partial\phi/\partial B)$ of about 10^{-10} G/ $\sqrt{\text{Hz}}$, which is comparable to the best values estimated in e.g. Ref. [4]. It is important to note that this high sensitivity is achieved in our case *despite more than three orders of magnitude difference* of the “natural” width of the Zeeman coherence γ_0 . This demonstrates the very significant potential of the present technique.

We now turn to a theoretical consideration of this result. As a simple model, let us consider the interaction of a dense ensemble of atoms with ground-state angular momentum $F = 1$ and an excited state $F = 0$ as shown in Fig. 3. (Although the calculation presented in Fig. 4 represents a simulation of realistic rubidium hyperfine structure, this simple model, with well-chosen parameters, represents the qualitative physics quite well.) We consider a strong laser tuned to exact resonance with the atomic transition and disregard inhomogeneous broadening. RCP and LCP intensities are then attenuated equally according to:

$$\frac{1}{P} \frac{dP}{dz} = \kappa \gamma \frac{[2|\Omega|^2 \gamma_0 + \gamma(4\delta^2 + \gamma_0^2)] \Delta \rho}{(2|\Omega|^2 + \gamma \gamma_0 - 2\delta^2)^2 + \delta^2(2\gamma + \gamma_0)^2}, \quad (3)$$

$$\frac{d\phi_{\pm}}{dz} = \pm \frac{\kappa \gamma \delta}{2} \frac{[4|\Omega|^2 - 4\delta^2 - \gamma_0^2] \Delta \rho}{(2|\Omega|^2 + \gamma \gamma_0 - 2\delta^2)^2 + \delta^2(2\gamma + \gamma_0)^2}, \quad (4)$$

where $\Omega = \wp|E_{\pm}|/\hbar$ are the (equal) Rabi frequencies of the field components ($P \propto |\Omega|^2$), γ_0 and γ are the relaxation rate of Zeeman and optical coherences respectively, $\delta = g\mu_B B/\hbar$ is the Zeeman level shift caused by an magnetic field B (g is a Landé factor), and $\kappa = 3/(4\pi)N\lambda^2(\gamma_{a \rightarrow b}/\gamma)$ is the weak field absorption coefficient (inverse absorption length), and $\gamma_{a \rightarrow b}$ is the natural width of the resonance. The population difference between the ground-state Zeeman sublevels and the upper state is $\Delta\rho$. This quantity is affected by optical pumping into the decoupled states (b_0 in Fig. 3), and depends upon cross-relaxation rates and applied magnetic field. For a weak magnetic field, $\Delta\rho \approx 1/3$.

One recognizes from Eq. (4) that in the case of optically thin media ($\kappa L \leq 1$ where L is the cell length) the phase shifts ϕ_{\pm} can be approximated by dispersive Lorentzian functions of δ , with amplitude $\phi_{max} = \kappa L \Omega^2 / (2\Omega^2 + \gamma \gamma_0) \Delta\rho$ and width $\delta_0 = \gamma_0/2 + \Omega^2/\gamma$. The former is typically rather small (on the order of mrad in the experiments of Ref. [1,2,4,8–11]) while the latter saturates when $|\Omega|^2$ exceeds the product $\gamma \gamma_0/2$, which corresponds to the usual power-broadening of the magneto-optic resonance [4,9].

It is important to emphasize here that a principal difference between regimes involving low and high driving power lies in the degree of Zeeman coherence excited by the optical field:

$$\rho_{b-b_+} = \frac{2|\Omega|^2 \Delta\rho}{2|\Omega|^2 + \gamma \gamma_0 - 2\delta^2 + i\delta(2\gamma + \gamma_0)} \quad (5)$$

Large coherence corresponds to a large population difference between symmetric (i.e. “bright”) and antisymmetric (i.e. “dark”) superpositions of Zeeman sublevels. In the low-power regime this difference is small corresponding to a small coherence. In a regime where the width of the resonance is determined by saturation, a very large (nearly maximal) Zeeman coherence is generated, as per Eq.(5).

We will now show that in a medium with large Zeeman coherence the magneto-optic

signal is maximized if a large density-length product is chosen. In the case of a strong optical field ($|\Omega|^2 \gg \gamma_0\gamma$) and weak magnetic fields $|\delta| < |\Omega|^2/\gamma, \sqrt{\gamma_0/\gamma}|\Omega|$, integration of Eqs. (3) and (4) yields for the transmitted power and the rotation angle $\phi = (\phi_+ - \phi_-)/2$

$$P(L) = (1 - \alpha_0 L) P(0) \quad (6)$$

$$\phi(L) = \frac{\delta}{2\gamma_0} \ln \left[\frac{1}{1 - \alpha_0 L} \right] \quad (7)$$

where $\alpha_0 = \Delta\rho \kappa\gamma\gamma_0/2|\Omega_0|^2$, and Ω_0 corresponds to the input field.

Note that in the case of a strong input field and an optically thin medium $\alpha_0 L \ll 1$. However Eq. (7) shows that maximal rotation is achieved with a large density-length product $\alpha_0 L$. Clearly $\alpha_0 L$ cannot be too close to unity, since then no light would be transmitted. Using Eq. (2) one finds the optimum value $(\alpha_0 L)_{opt} = 1 - e^{-2}$, corresponding to a density-length product

$$\Delta\rho\kappa L|_{opt} = (\alpha_0 L)_{opt} \frac{|\Omega_0|^2}{\gamma\gamma_0} \gg 1. \quad (8)$$

In this case the total accumulated rotation angle is quite large and the slope of its dependence upon B is maximal:

$$\partial\phi_{opt}/\partial B = g\mu_B/(\hbar\gamma_0) \quad (9)$$

which is in strikingly good agreement with our measured value. The significance of this result can be understood by noting that in a shot-noise limited measurement, the minimum detectable rotation ϕ_{err} given in Eq. (2) is inversely proportional to the square root of the laser power. Working at high power, therefore, has a clear advantage, since the fundamental shot noise error is reduced even though the signal is large.

To make a more realistic comparison of theory and experiment, we have carried out detailed calculations in which coupled density matrix and Maxwell equations including propagation through the medium and Doppler broadening have been solved numerically for the two components of the optical field. The calculation takes into account a 16-state atomic system with energy levels and coupling coefficients corresponding to those of the Rb D_1 line.

The results of these calculations are shown in Fig. 4 and are in good agreement with the experimental results. In particular, we note that our calculations predict the maximal rotation angle, (which is apparently limited by the optical pumping into the $F=1$ $S_{1/2}$ hyperfine manifold) as well as the slope of the resonance curve.

It is important to comment at this point on possible limitations for the extension of the present technique into the domain of narrow resonances. For instance, in the case of a long-lived ground state coherence, spin-exchange collisions can become a limiting factor for the Zeeman relaxation rate. In the case of Rb, this is a few tens of Hz at densities corresponding to the present operating conditions. We note however that it is possible to operate at lower densities by increasing the optical path length (e.g. by utilizing an optical cavity). Likewise, the role of the light shifts due to off-resonant coupling to e.g. $F=1$ $S_{1/2}$ and $F=2$ $P_{1/2}$ hyperfine manifolds needs to be clarified. Although the noise due to classical intensity fluctuations of the circular components of the optical field is obviously canceled in a measurement of the polarization rotation, there might exist additional quantum contributions that add noise. We note however that even if such contributions are present, it is likely that they can be suppressed by tuning the laser to the point of minimum light shifts.

For these reasons, we believe that the combination of the present approach with buffer gas or wall-coating techniques is likely to improve substantially the sensitivity of nonlinear magneto-optical measurements. Therefore, we anticipate that this method will be of interest for sensitive optical magnetometry as well as for setting new, lower bounds in test for the violation of parity and time-reversal invariance [3,4].

The authors warmly thank Leo Hollberg, Alexander Zibrov, and Michael Kash for useful discussions and Tamara Zibrova for valuable assistance. We gratefully acknowledge the support of the Office of Naval Research, the National Science Foundation, the Welch Foundation, and the Air Force Research Laboratory.

REFERENCES

- [1] W. Gawlik, J. Kowalski, R. Neumann, and F. Träger, Phys. Lett. **A48**, 283 (1974); W. Gawlik, in *Modern Nonlinear Optics*, part 3, M. Evans and S. Kielich, eds., Wiley (1994).
- [2] K. H. Drake, W. Lange, and J. Mlynek, Opt. Comm. **66**, 315 (1988).
- [3] E. A. Hinds, *Atomic Physics* Vol.11 (1988), S. Haroche, J. C. Gray and G. Grynberg, Eds.; L. R. Hunter, Science **252**, 73 (1991).
- [4] D. Budker, V. Yashchuk, and M. Zolotarev, Phys. Rev. Lett. **81**, 5788 (1998); V. Yashchuk et al., preprint LBNL-42228 (1998); This work is performed off-resonance to avoid the rather stringent limitations on the width due to power broadening. This approach yields a reduction in the width of the dispersive feature but it also results in a decreased amplitude of the resonances. As a consequence, the magneto-optical signal (rotation angle per applied magnetic field) decreases with detuning from the line center.
- [5] S. E. Harris, Physics Today **50**, 36 (1997).
- [6] Applications of EIT for polarization control and birefringence have been discussed in F. S. Pavone, G. Bianchini, F. S. Cataliotti, T. W. Hänsch, and M. Inguscio, Opt. Lett. **22**, 736 (1997); S. Wielandy and A. Gaeta, Phys. Rev. Lett. **81**, 3359 (1998).
- [7] S. Giraud-Cotton et al., Phys. Rev. A **32**, 2211 (1985), *ibid* 2223 (1985); F. Schuller et al., *ibid* **71**, 61 (1989).
- [8] L. M. Barkov, D. Melik-Pashayev, and M. Zolotarev, Opt. Comm. **70**, 467 (1989);
- [9] A. Weis, V. A. Sautenkov, and T. W. Hänsch, Phys. Rev. A **45**, 7991 (1992)
- [10] S. I. Kanorsky, A. Weis, J. Wurster, and T. W. Hänsch, Phys. Rev. A **47**, 1220 (1993).
- [11] S. I. Kanorsky, J. Scalla, and A. Weis, Appl. Phys. **B60**, S165 (1995).
- [12] E. Arimondo, *Progress in Optics XXXV*, 259-354 (1996).

- [13] S. Brandt, A. Nagel, R. Wynands, and D. Meschede, Phys. Rev. A **56**, R1063 (1997).
- [14] M. Lukin et al., Phys. Rev. Lett. **79**, 2959 (1997).
- [15] M. O. Scully and M. Fleischhauer, Phys. Rev. Lett. **69**, 1360 (1992).
- [16] L. V. Hau, S. E. Harris, Z. Dutton, and C. H. Behroozi, Nature **397**, 594 (1999).

FIGURES

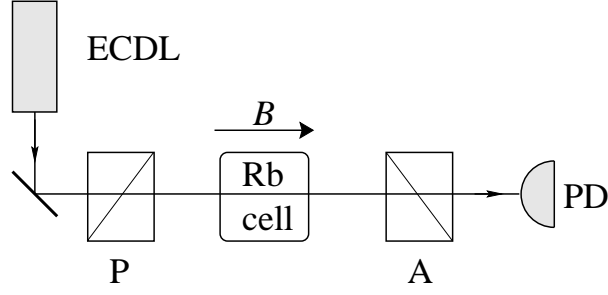


FIG. 1. Schematic of the experimental setup. The laser beam passes through polarizer (P), Rb cell, and analyzer (A) and is detected by the photodiode (PD).

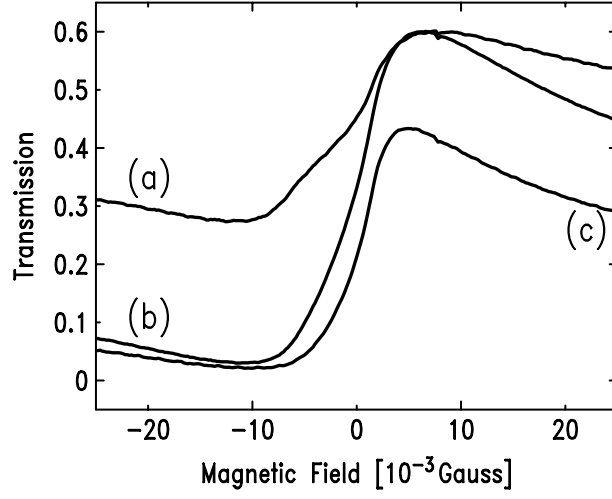


FIG. 2. Experimentally measured transmission through the system of Fig. 1 where the polarizer axes are 45° apart. The vertical scale is normalized such that unity corresponds to the transmission of the laser beam in the absence of the atomic cell and the polarizers. Thus, zero magnetic field at low density gives a transmission through the system of 50%. Curves (a-c) correspond to increasing atomic density: (a) $N = 3 \times 10^{11} \text{ cm}^{-3}$, (b) $N = 1 \times 10^{12}$, (c) $N = 2 \times 10^{12}$.

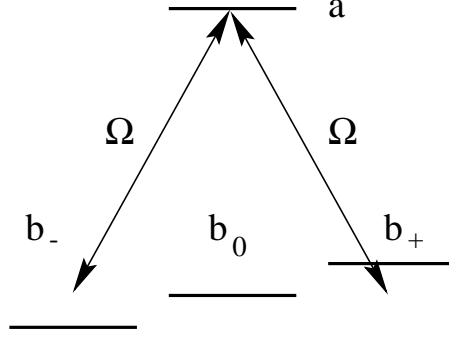


FIG. 3. A simplified, four-state model for observation of nonlinear Faraday effect. Ω is the Rabi-frequency of $\hat{\sigma}_{\pm}$ components of an \hat{x} -polarized laser field. The magnetic field B shifts $m = \pm 1$ levels by $\pm\delta$.

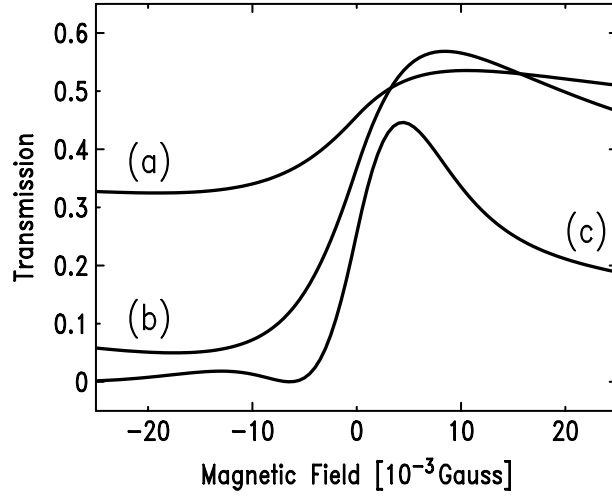


FIG. 4. Results of numerical simulations with parameters corresponding to Fig. 2.